

Figure S1

Figure S1. *P. aeruginosa* toxin engages EGFR pathway, independent of receptor endocytosis or MyD88, to stimulate epithelial cells, Related to Figure 1

(A) (Left) Inhibition of LasB activity with phosphoramidon using *in vitro* elastin cleavage assay. IC50 is shown in inset box (n=5). (Right) Elastase activity of purified recombinant LasB with increasing concentrations of LasB inhibitor, phosphoramidon (n=3).

(B) Expression of recombinant *P. aeruginosa* (PA01) 6XHis-tagged LasB in *E. coli*. LasB expression was induced by addition of 0.4 mM IPTG for 2 hr at 37 °C (n=3).

(C) First-step chromatography of recombinant LasB on Ni-NTA column. LasB expression was induced by addition of 0.2 mM IPTG into 200 ml of *E. coli* cell culture for 4 hrs. FH – flow through fraction.

(D) Second step chromatography of recombinant LasB on ion-exchange MonoQ column.

(E) Relative mRNA expression of TSLP and Areg (top) and immunoblot analysis of P-S6 in H292 cells stimulated with EGF (50 ng/ml) +/- EGFR inhibitor (EGFR Inh., 20 µM), LasB inhibitor (Phdon, 50 µM) for 3 hr (n=4).

(F) Immunoblot analysis of P-EGFR Tyr1068 and P-S6 in H292 cells stimulated with LasB (5 µg/ml) and EGF (10 ng/ml) for indicated times (n=3).

(G) Relative mRNA expression of pro-inflammatory (IL-1α, IL-8) and tissue repair (TSLP, Areg) genes in H292 cells treated with commercial and recombinant in-house LasB (2 µg/ml) for 3 hr (n=2).

(H) Relative mRNA expression of pro-inflammatory (IL-1α, IL-8) and tissue repair (TSLP, Areg) cytokine genes in H292 cells treated with recombinant in-house LasB (2 µg/ml) +/- inhibitor (50 µM) for 3 hr (n=2).

(I and J) Immunoblot analysis of P-S6 (I) and relative mRNA expression of TSLP and Areg (J) in H292 cells treated with control, AP2M or PACSIN3 siRNA and stimulated with LasB (5 µg/ml) and papain (8 µg/ml) for 3hr (n=2). I left – immunoblot analysis of P-S6 in H292 cells treated with “control” (targeting EGFR), Par1, Par2 or IGFR siRNA.

(K) Relative mRNA expression of TSLP and Areg in H292 cells treated with control or MyD88 siRNA and stimulated with LasB (5 µg/ml) or flagellin (10 µg/ml) for 3hr (n=4).

(L) Immunoblot analysis of P-p44/42 MAPK (left) and relative mRNA expression of TSLP, Areg, EGFR and PAR-2 (right) in H292 cells treated with control and PAR-2 siRNA and stimulated with LasB (5 µg/ml) or Trypsin (25 nM) (n=4).

mRNA expression was measured relative to HMGN4. β-actin was used as loading control. n = independent experiments. Data are mean ± SD and were analyzed by one-way ANOVA with Tukey's multiple comparisons test (A, E) or two-tailed unpaired Student's t test (K, L). *p < 0.05; **p < 0.01; ***p < 0.001; ****p < 0.0001.

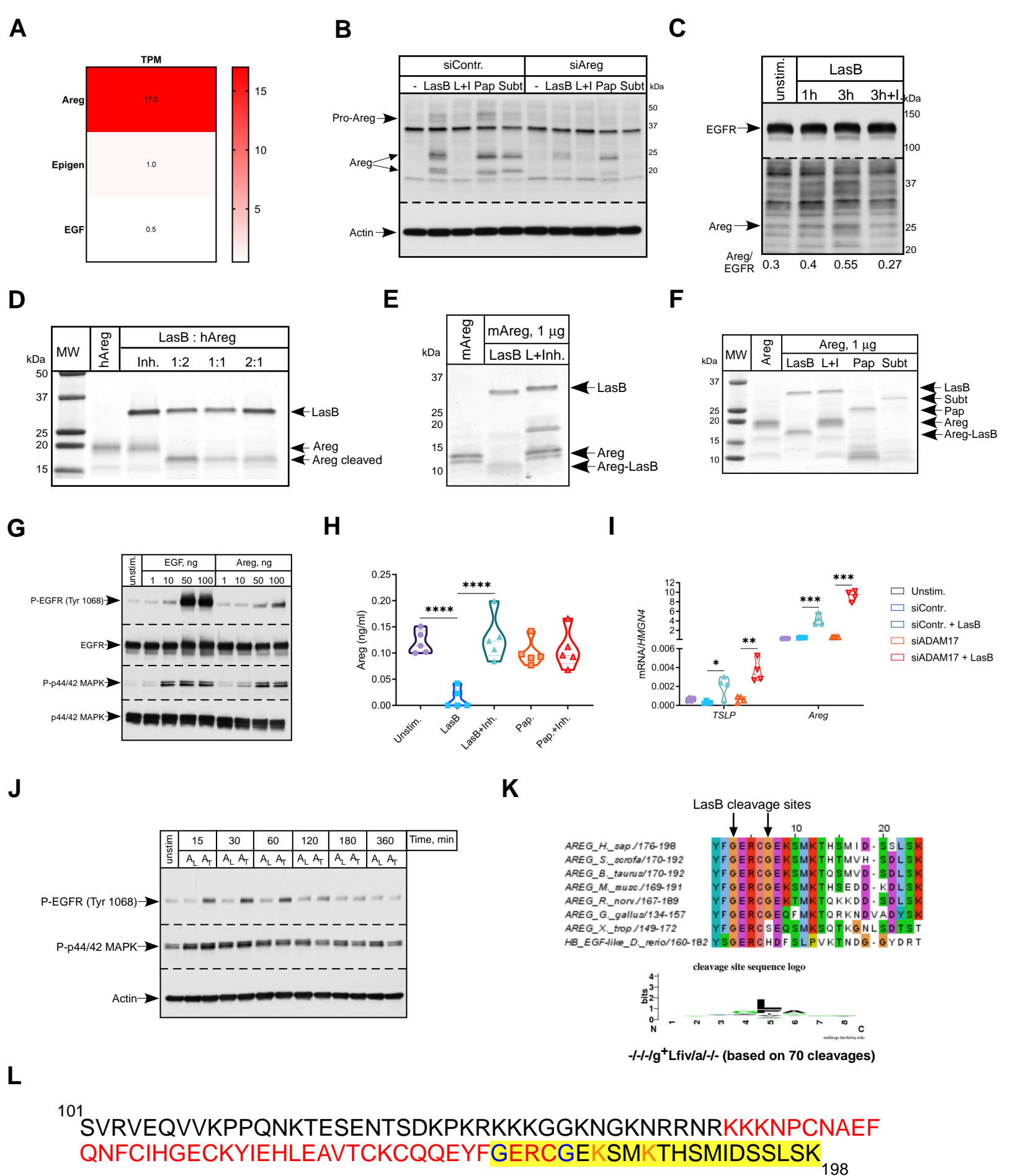


Figure S2

Figure S2. *P. aeruginosa* toxin utilizes amphiregulin to activate epithelial cells, Related to Figure 2

(A) TPM of EGF-family ligands from RNA-seq of 675 commonly used human cancer cell lines (Klijn et al., 2015).

(B) Immunoblot analysis of Areg in H292 cells treated with control or Areg siRNA and stimulated with LasB (5 µg/ml) +/- inhibitor (50 µM), papain (8 µg/ml) or subtilisin (1 µg/ml) for 3hr (n=3).

(C) Immunoblot analysis of Areg in input samples before immunoprecipitation with anti-EGFR antibodies in H292 cells stimulated with LasB (3 µg/ml) +/- inhibitor (50 µM) (n=3).

(D) *In vitro* cleavage of recombinant human Areg by LasB. Ratios (in µg) of recombinant human Areg to LasB (1:2, 1:1, 2:1) +/- inhibitor (50 µM) were used (n=7).

(E and F) *In vitro* cleavage of recombinant mouse (E) or human (F) Areg (1 µg) by LasB (0.5 µg) +/- inhibitor (50 µM), papain and subtilisin (both 0.5 µg) (n=3-5).

(G) Immunoblot analysis of P-EGFR Tyr1068 and P-p44/42 MAPK in H292 cells treated with indicated amounts of EGF or Areg for 1hr (n=3).

(H) ELISA of Areg amounts in H292 cell supernatants pre-treated with LasB or papain inhibitor (both 50 µM) for 10-15 min and stimulated with LasB (2 µg/ml) or papain (8 µg/ml) for 3hr (n=5).

(I) Relative mRNA expression of TSLP and Areg in H292 treated with control or ADAM17 or TACE siRNA and stimulated with LasB (2 µg/ml) for 3hr (n=4).

(J) Immunoblot analysis of P-EGFR Tyr 1068 and P-p44/42 MAPK in H292 cells stimulated with A_L or A_T (50 ng/ml) (n=3).

(K) Sequence alignment of Areg from different species (top) and cleavage site sequence for LasB based on MEROPS database (bottom) (Rawlings et al., 2018). EGF-like domain containing LasB cleavage sites was used for alignment. LasB cleavages sites are shown by arrows.

(L) Sequence of recombinant human Areg with depicted cleavage sites for ADAM17 or TACE (K184 and K187 in orange) and LasB (G178 and G182 in blue). EGF-like domain is highlighted in red. Areg peptide likely cleaved by LasB is highlighted in yellow box.

mRNA expression was measured relative to HMGN4. β-actin, total EGFR and p44/42 MAPK were used as loading controls. n = independent experiments. Data were analyzed by one-way ANOVA with Tukey's multiple comparisons test (H, I). *p < 0.05; **p < 0.01; ***p < 0.001, ****p < 0.0001.

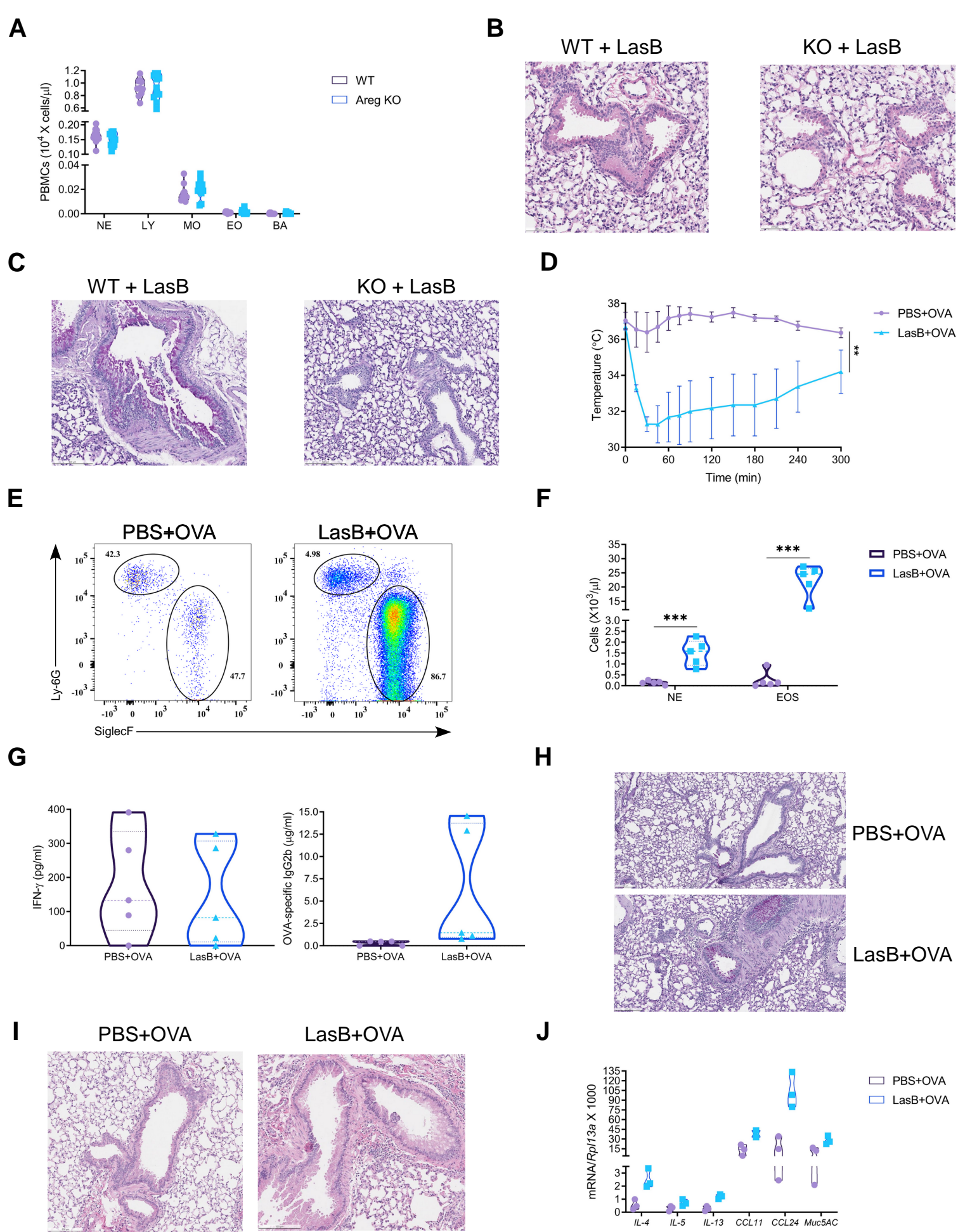


Figure S3

Figure S3. LasB is an adjuvant for allergic response, Related to Figures 3 and 4

(A) Analysis of PBMCs counts in WT and *Areg*^{-/-} (KO) mice at basal state (combined of 2 experiments yielding 10-11 mice per group).

(B and C) H&E (B, scale bar = 200 μ m) and PAS (C, scale bar = 500 μ m) staining in the lungs of LasB-challenged WT and *Areg*^{-/-} (KO) mice in innate airway inflammation model (representative of 3 experiments, 3-5 mice per group).

(D) Rectal temperature measurements of mice immunized with OVA +/- LasB in airway allergic inflammation model (combined of 2 experiments yielding 6 mice per group).

(E and F) Representative FACS plots (n=2) (E) and graphs showing cell numbers (F) of eosinophils (CD45+MHCII-CD11b+Siglec-F+) and neutrophils (CD45+MHCII-CD11b+Ly6G+) out of CD45+ cells in the BAL of mice immunized as in (D) (combined of 2 experiments yielding 5 mice per group).

(G) ELISA of IFN-g in the BAL (left) and OVA-IgG2b in the serum (right) of mice immunized with OVA +/- LasB (combined of 2 experiments yielding 5 mice per group).

(H and I) PAS (H) and H&E (I) staining in the lungs of mice immunized as in (D) (representative of 3 experiments, 3 mice per group, scale bar = 500 μ m).

(J) Relative mRNA expression of type 2 cytokines (IL-4, 5, 13), eotaxins (Ccl11, 24) and Muc5AC in the lungs of mice immunized as in (D) (representative of 3 experiments, 3 mice per group).

Data are mean \pm SD and were analyzed by two-tailed unpaired Student's t test or one-way ANOVA (D). **p < 0.01; ***p < 0.001.

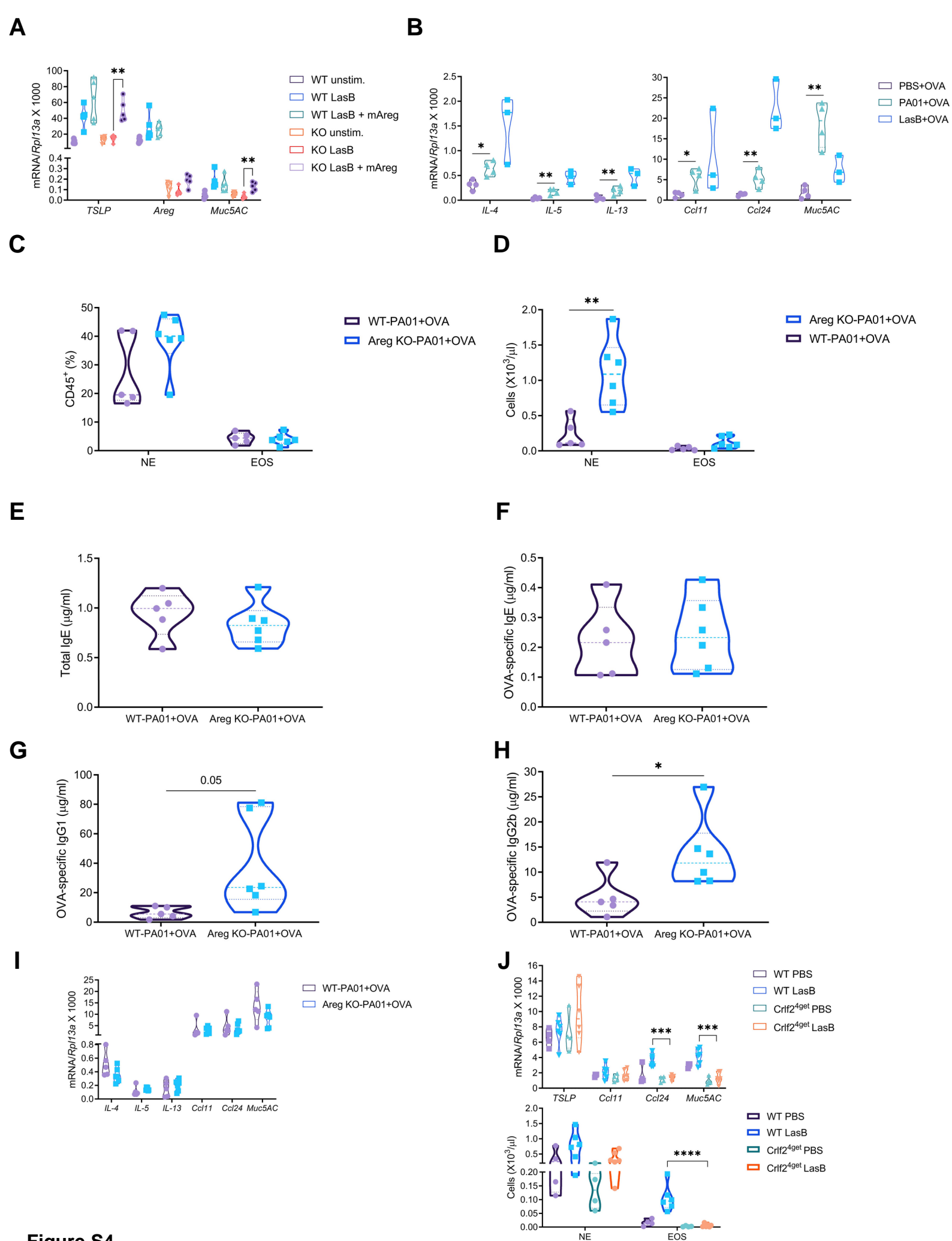


Figure S4. *P. aeruginosa* can serve as an adjuvant for an allergic response, Related to Figure 3 and 5

(A) Relative mRNA expression of TSLP, Areg and Muc5AC in WT and *Areg*^{-/-} (KO) mouse lung organ cultures stimulated with LasB (5 µg/ml) +/- mAreg (10 ng/ml) for 8 hr (n=5).

(B) Relative mRNA expression of type 2 cytokines (IL-4, 5, 13), eotaxins (Ccl11, 24) and Muc5AC (from left to right) in the lungs of mice immunized with OVA +/- WT PA01 or LasB (representative of 3 experiments, 3-4 mice per group).

(C and D) Cell frequency (B) and numbers (C) of eosinophils (CD45+MHCII-CD11b+CD64-Siglec-F+) and neutrophils (CD45+MHCII-CD11b+CD64-Ly6G+) out of CD45+ cells in the BAL of WT and *Areg*^{-/-} (KO) mice immunized with OVA +/- WT PA01.

(E-H) ELISA of total IgE (E), OVA-specific IgE (F), OVA-specific IgG1 (G) and OVA-specific IgG2b (H) in the serum of WT and *Areg*^{-/-} (KO) mice immunized as in (C and D).

(I) Relative mRNA expression of type 2 cytokines (IL-4, 5, 13), eotaxins (Ccl11, 24) and Muc5AC in the lungs of mice immunized as in (C and D).

(J) (Top) Relative mRNA expression of *Tslp*, *Ccl11*, *Ccl24* and *Muc5AC* in the lungs of LasB-treated WT and *Crlf2*^{4get} mice and (bottom) graphs showing cell numbers of eosinophils (CD45+MHCII-CD11b+Siglec-F+) and neutrophils (CD45+MHCII-CD11b+Ly6G+) out of CD45+ cells in the BAL of LasB-treated WT and *Crlf2*^{4get} mice (combined of 2 experiments yielding 4-6 mice per group).

For (C-I) representative of 2 experiments, 5-6 mice per group. mRNA expression was measured relative to *Rpl13a*. n = independent experiments. Data were analyzed by two-tailed unpaired Student's t test and one-way ANOVA with Tukey's multiple comparisons test (J). *p < 0.05; **p < 0.01, ***p < 0.01, ****p < 0.001.

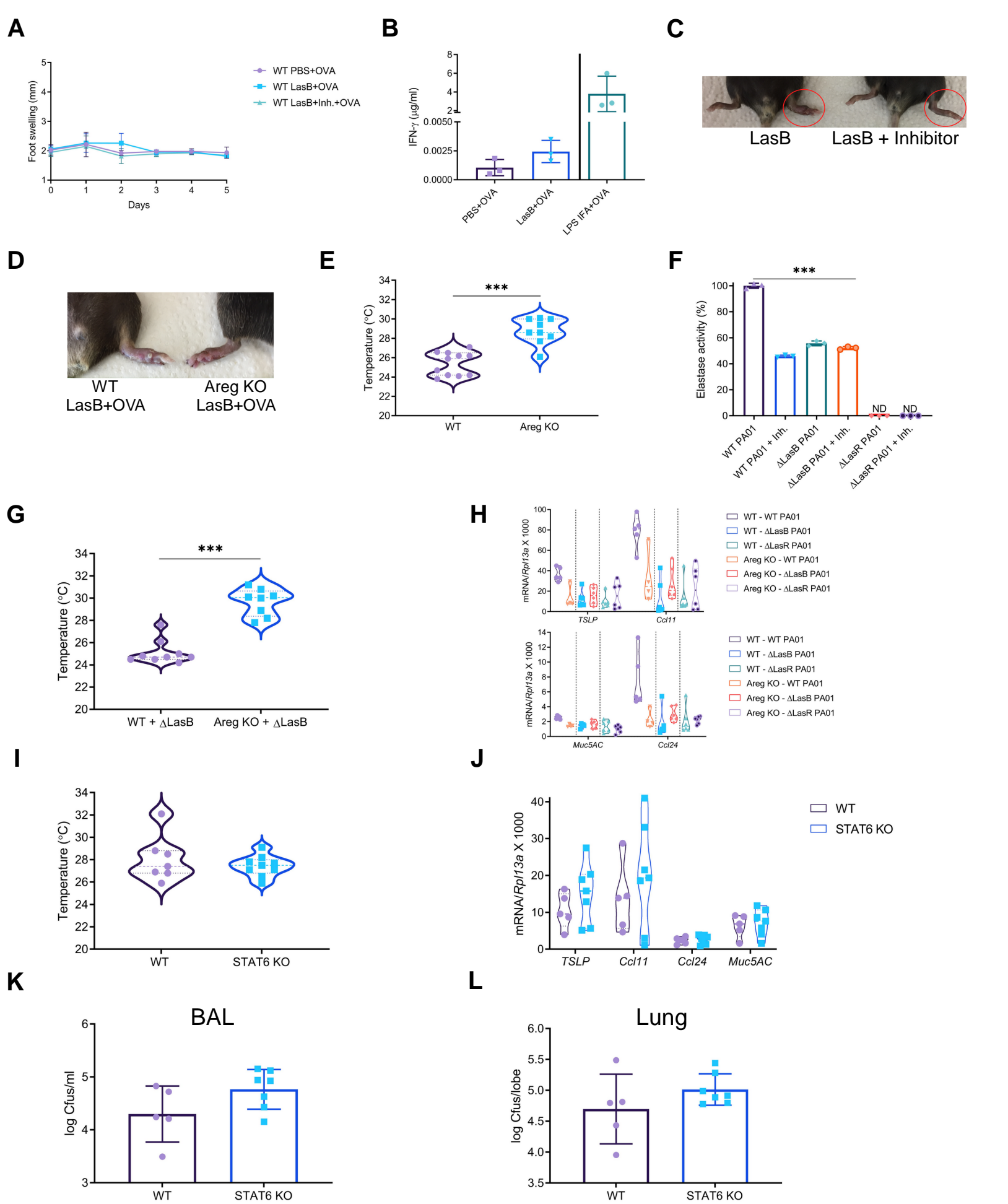


Figure S5

Figure S5. Amphiregulin is required for successful *P. aeruginosa* infection, Related to Figures 4 and 6

(A) Kinetics of swelling in non-injected right footpad of mice immunized with LasB+OVA +/- inhibitor in skin allergic inflammation model (combined of 2 experiments yielding 3-6 mice per group).

(B) IFN γ production after *ex vivo* stimulation of total lymph node cells from mice immunized as in (A) or with LPS and IFA and OVA (representative of 2 experiments, 3 mice per group).

(C and D) Photograph of left hind footpads of WT mice (C) or WT and *Areg*^{-/-} (KO) mice (D) immunized with LasB+OVA +/- inhibitor.

(E) Temperature measurements of WT and *Areg*^{-/-} (KO) mice 12 hr after WT PA01 infection (combined of 2 experiments yielding 9-11 mice per group).

(F) Elastase activity measurements in supernatants collected from WT, Δ LasB and Δ LasR PA01 cell cultures (n=3).

(G) Temperature measurements of WT and *Areg*^{-/-} (KO) mice 12 hr after infection with Δ LasB PA01 (combined of 2 experiments yielding 8-9 mice per group).

(H) Relative mRNA expression of TSLP, eotaxins (Ccl11, 24) and Muc5AC in the lungs of WT and *Areg*^{-/-} (KO) mice infected with WT, Δ LasB or Δ LasR PA01 for 12 hr (representative of 3 experiments, 4-6 mice per group).

(I) Temperature measurements of WT and *STAT6*^{-/-} (KO) mice 12 hr after WT PA01 infection (combined of 2 experiments yielding 7-9 mice per group).

(J) Relative mRNA expression of TSLP, eotaxins (Ccl11, 24) and Muc5AC in the lungs of WT and *STAT6*^{-/-} (KO) mice infected with WT PA01 for 12 hr.

(K and L) BAL (K) and lung (L) bacterial load of WT PA01 in WT and *STAT6*^{-/-} (KO) mice 12 hr after infection. J-L - representative of 3 experiments, 5-7 mice per group. mRNA expression was measured relative to Rpl13a. Data are mean \pm SD and were analyzed by two-tailed unpaired Student's t test or one-way ANOVA with Tukey's multiple comparisons test (F). ***p < 0.001.

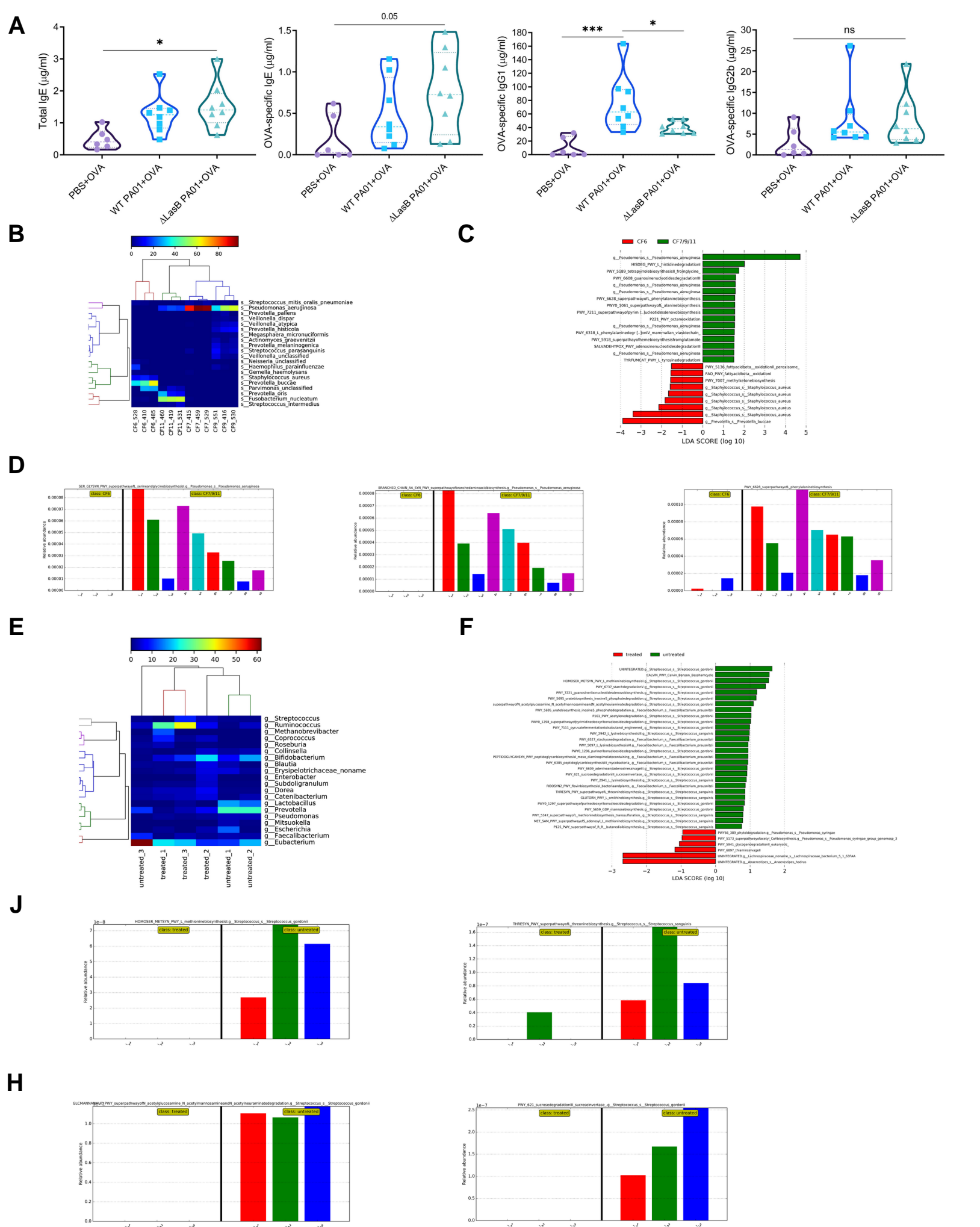


Figure S6

Figure S6. Human lung and gut microbiomes use known mucin utilization pathways under conditions mimicking type-2 response, Related to Figure 7

(A) ELISA of total IgE, OVA-specific IgE, IgG1, IgG2b (from left to right) in the serum of mice immunized with OVA +/- WT or Δ LasB PA01 (combined of 2 experiments yielding 6-8 mice per group, analyzed by one-way ANOVA with Tukey's multiple comparisons test, * $p < 0.05$; *** $p < 0.001$).

(B) Taxonomic classification of the lung microbiome of cystic fibrosis patients at different stages of disease.

(C) Histogram of the linear discriminant analysis (LDA) scores computed for differentially abundant microbiome metabolic pathways (based on HUMAnN2) of cystic fibrosis patients colonized (CF7/9/11) vs non-colonized (CF6) with *P. aeruginosa*.

(D) Histogram of the relative abundances of the metabolic pathways (from left to right – serine and glycine, branched chain amino acids and phenylalanine biosynthesis) in the lung microbiome of cystic fibrosis patients colonized (CF7/9/11) vs non-colonized (CF6) with *P. aeruginosa*. Classes (patients) are shown in the top of the histograms. Subclasses (individual patient samples at different stages of disease) are differentially colored, and the relative abundances of the pathways are indicated.

(E) Taxonomic classification of the fecal microbiome of worm-infected patients treated vs non-treated with anthelmintics.

(F) Histogram of the LDA scores computed for differentially abundant microbiome metabolic pathways (based on HUMAnN2) between worm-infected patients treated vs non-treated with anthelmintic.

(G and H) Histogram of the relative abundances of the amino acid biosynthesis (G) and polysaccharide degradation (H) pathways in the fecal microbiome of worm-infected patients treated vs non-treated with anthelmintic. Classes (patients) are shown in the top of the histograms. Subclasses (individual patient samples) are differentially colored, and the relative abundances of the pathways are indicated.

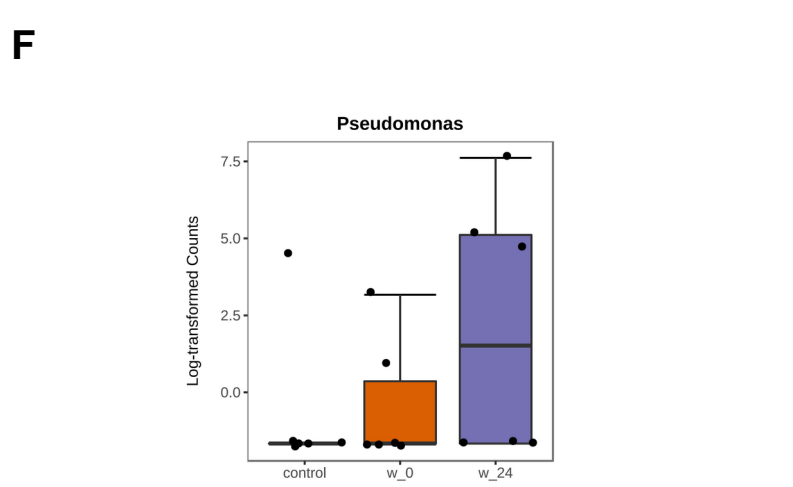
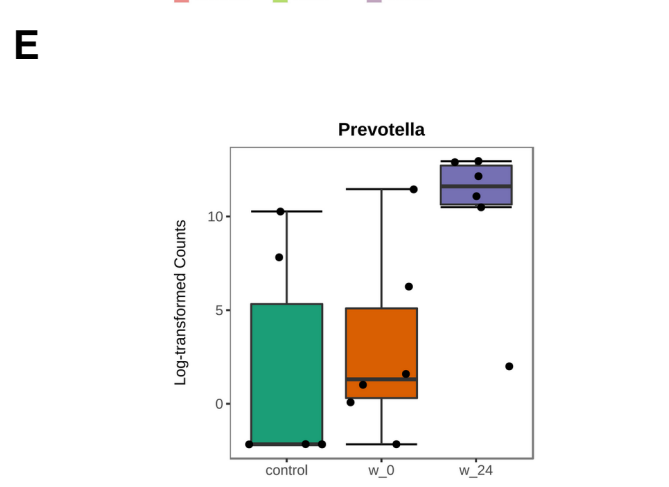
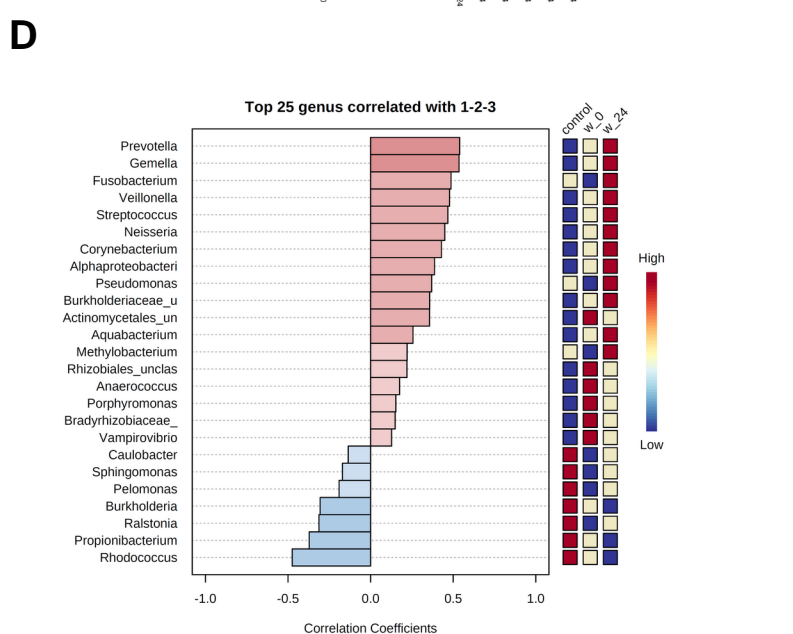
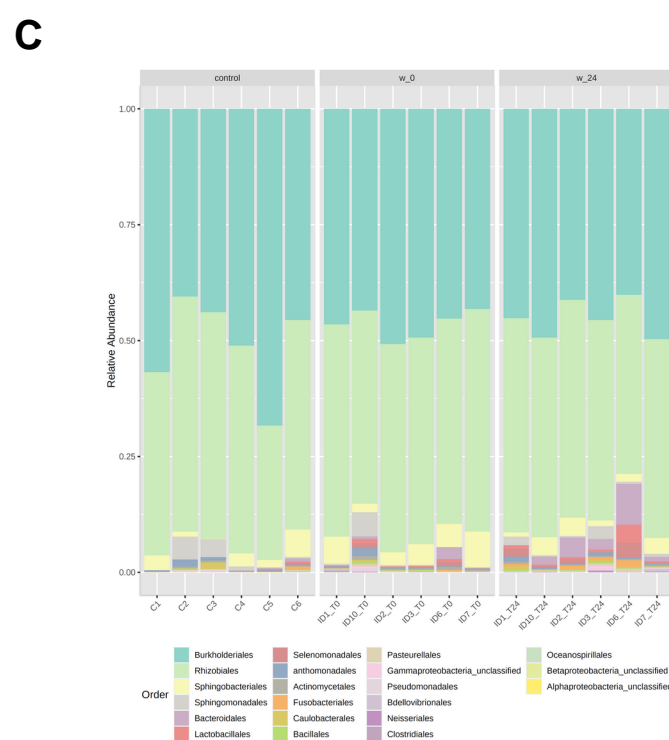
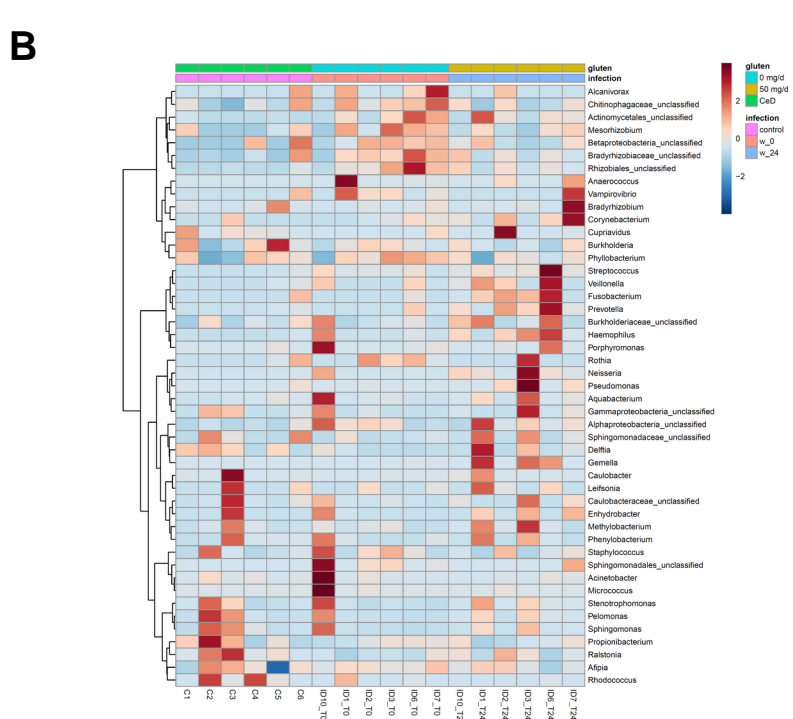
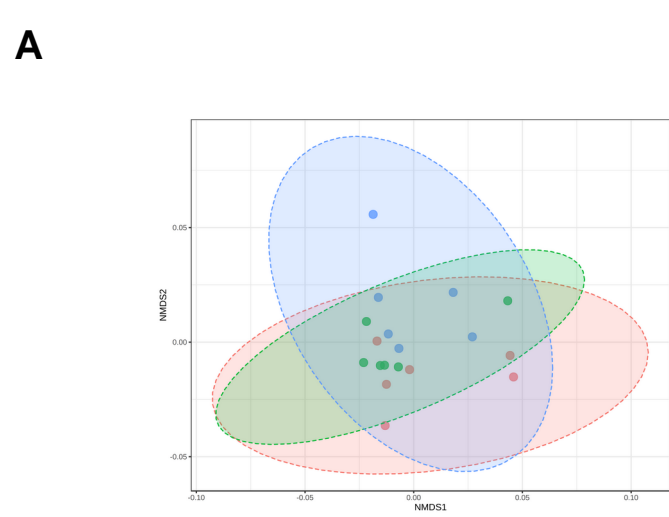


Figure S7

Figure S7. *Prevotella* and *Pseudomonas* species are enriched in duodenum of worm-infected celiac patients, Related to Figure 7

(A) β -diversity analysis of control, gluten-challenged uninfected or worm-infected celiac patients.

(B) Heatmap clustering of duodenal microbiome of celiac patients as in (A).

(C) Relative abundances of duodenal microbiome orders of celiac patients as in (A).

(D-F) Correlation analysis of duodenal microbiome at the level of different genera (D) and *Prevotella* (E – $r(\text{Pearson})=0.546$, $p=0.02$) or *Pseudomonas* (F – $r(\text{Pearson})=0.37$, $p=0.13$) genera of celiac patients as in (A).

Table S2. qPCR primers used in this study. Related to Figures 1-3, 6, 7 and S1-S5.

Gene name	Forward primer	Reverse primer
human <i>AREG</i>	TGATCCTCACAGCTGTTGCT	TCCATTCTCTTGTCTGAAGTTTCT
human <i>EGFR</i>	GGAGAACTGCCAGAACTGACC	GCCTGCAGCACTGGTTG
human <i>F2RL1</i> (<i>PAR-2</i>)	ATCTGGTTCCCCTTGAAGATTGC	G TTCACGACCCAATACCTC
human <i>IL-1a</i>	AAGCTGCAGCCAGAGAGGGA	AGCCTTCATGGAGTGGGCCATA
human <i>IL-8</i>	CCTGATTTCTGCAGCTCTGTGTG A	CACCCAGTTTTCTTGGGGTCCA
human <i>HMGN4</i>	GTCACGGGCCTCAGCTGGGAT	AGCAGTGTTTCGCAGGTGGCTT
human Muc5AC	CTATGTGCTGACCAAGCCCT	TCAGTGTACGCTCTTCAGG
human <i>TSLP</i>	AAAGTACCGAGTTCAACAAC	GTAGCATTTATCTGAGTTTCCG
mouse <i>AREG</i>	ATCACAGTGCACCTTTGGAAAC	GTCCCGTTTTCTTGTCTGAAGC
mouse <i>CCL11</i>	CTTCACCTCCCAGGTGCT	TTGTAGCTCTTCAGTAGTGTGTTG G
mouse <i>CCL24</i>	AGTGGTTAGCTACCAGTTGGC	CACTGCCTTGGCCCCTTTAG
mouse <i>IL-4</i>	CTGGATTCATCGATAAGCTG	TTTGCATGATGCTCTTTAGG
mouse <i>IL-5</i>	AGACTTCAGAGTCATGAGAAG	GCTGGTGATTTTTATGAGTAGG
mouse <i>IL-13</i>	CTTAAGGAGCTTATTGAGGAG	CATTGCAATTGGAGATGTTG
mouse Muc5AC	CCATGCAGAGTCCTCAGAACAA	T TACTGGAAAGGCCCAAGCA
mouse <i>RPL13a</i>	GAGGTCGGGTGGAAGTACCA	TGCATCTTGGCCTTTTCCTT
mouse <i>TSLP</i>	TCAATCCTATCCCTGGCTGC	GCCATTTCTGAGTACCGTCA

Table S3. Patient demographics. Related to Figure 7 and STAR Methods Bacterial growth on Muc5AC and human sputum samples.

Patient#	Sex	Age	Race
1	M	60	Caucasian
2	M	20	African American
3	F	69	Caucasian
4	M	37	Caucasian